Polymer Bulletin (2020) 77:4147–4166
https://doi.org/10.1007/s00289-019-02966-x

ORIGINAL PAPER

PVGA/Alginate-AgNPs hydrogel as absorbent biomaterial and its soil biodegradation behavior

G. M. Estrada-Villegas[1] · G. Morselli[2] · M. J. A. Oliveira[2] · G. González-Pérez[1,2] · A. B. Lugão[2]

Received: 24 April 2019 / Revised: 1 July 2019 / Accepted: 17 September 2019 /
Published online: 20 September 2019

Abstract

PVGA, silver nitrate ($AgNO_3$) and alginate (Alg) were cross-linked by using γ-ray radiation to obtain Alg/PVGA/AgNPs as a potential biomaterial. The hydrogel composition was characterized by several analytics methods, and the morphology was evaluated by scanning electron microscopy. The swelling behavior was tested in different mediums. The stability of AgNPs was followed by UV–Vis at 400 nm for 1 month. The hydrogel soil biodegradation was analyzed by visual observation, weight loss, Fourier transform infrared spectroscopy and thermogravimetric analysis for 120 days. A simple biodegradation mechanism has been proposed based on results. Additionally, cytotoxicity assays were carried out using NCTC 929 cells to observe cell viability.

Keywords Biomaterial · Cross-linking · Biodegradation · Hydrogel · Silver nanoparticles

Introduction

Hydrogels are cross-linked hydrophilic polymers forming three-dimensional networks, capable of absorbing and retaining a large volume of water in aqueous environments [1, 2], which allow a vast range of applications in biomedical, agricultural, veterinary and pharmaceutical areas [3]. The biomaterials used for wound dressings require proper exudates absorption, the maintenance of a moist environment around the wound and the protection of surrounding skin from maceration [4]. Therefore, hydrogels also exhibit the desired properties for wound dressing applications [5].

✉ G. M. Estrada-Villegas
mayeli.estrada@ciqa.edu.mx

[1] CONACyT–Centro de Investigación en Química Aplicada, Av. Alianza Sur 204 Parque de Innovación e Investigación Tecnológica, 66629 Apodaca, Nuevo León, Mexico

[2] CQMA-Nuclear and Energetic Research Institute IPEN-CNEN, Sao Paulo, SP 05508-000, Brazil

Polymer modification by blends is a practice route to obtain new materials with better properties, such as biodegradability, which is liable to prevent solid waste and environment pollution [3, 6]. A synthetic polymeric matrix can have this property achieved or improved by the physical incorporation of a natural polymer, since it possesses unique characteristics as specific recognition of molecules and formation of reversible bonds, in addition to the inherent biodegradability [3, 7, 8]. When integrated into the soil after their lifespan, biodegradable materials are transformed into carbon dioxide or methane, water and biomass by bacterial flora [9]. This process can be monitored by evaluating parameters such as CO_2 formation, biochemical oxygen demand (BOD) and weight loss [10]. Tudorachi [11] and Salehpour [6] have done weight loss determination studies in agar–agar-based solid medium and in solid waste composting for a PVA-starch-based polymer and cellulose-based nanocomposites, respectively; this is a simple method that offers an excellent overview of the biodegradation process. Also, degradation intermediate products can be monitored by techniques as FTIR spectroscopy.

Sodium carboxymethyl cellulose (CMC) [12], starch [11], cellulose [13] and chitosan [14] are examples of natural polymers blended into synthetic polymeric materials to improve its biodegradability [15], as well as alginate, used mainly in biomedical applications [16]. Alginate is a term for alginic acid, its salts and its derivatives. It is a linear unbranched copolymer, naturally occurring in brown algae and consisting of two distinct monosaccharide residues ((1,4)-b-D-mannuronic acid (M) and (1,4)-a-L-guluronic acid (G)) [16, 17], which has a variety of applications such as superabsorbent fibers [17], wound dressings [18] and in the field of tissue engineering [19]. Many researchers developed PVA–alginate-based hydrogels aiming the wound dressing application, [18–20], but indeed, modified PVA by acetalization can improve the desired features of the hydrogel. Poly (vinyl glyoxylic acid) (PVGA) is the acetalization reaction product of glyoxylic acid or salt with two contiguous poly (vinyl alcohol) monomers. In our previous work [21], we reported an increment of 368% in the swelling behavior of radiation cross-linked PVGA/PVA (0.8) hydrogel compared to PVA one. The acetal group of the PVGA chains is highly hydrophilic and is responsible for the increment in swelling behavior.

There are examples in the literature of hydrogels containing different nanoparticles as a function of the desired application. Zinc oxide nanoparticles [19], gold nanoparticles [22], silicon nanoparticles [22], and silver nanoparticles [23] are examples of this practice. Polymer matrix containing silver nanoparticles (AgNPs) provides a sustained release of silver ion [23]. It is known that AgNPs have antimicrobial activity, even in nanomolar concentrations [24], and consequently, its incorporation in biomaterials is desirable since it acts against microbes—mainly bacteria—to avoid infections, besides being relatively non-toxic for human cells [25]. Chandran [26] encapsulated biosynthesized silver nanoparticles in a PVA matrix. Becaro [27] determined the toxicity of chemically synthesized silver nanoparticle stabilized by PVA to algae and microcrustaceans. Eghbalifam [28] synthesized antibacterial AgNPs in a polyvinyl alcohol/sodium alginate composite film by in situ gamma irradiation. El-Shamy [29] enhanced the conductivity and dielectric properties of PVA/Ag nanocomposite films using gamma radiation, and Swaroop [30] synthesized via gamma irradiation AgNPs/PVA hydrogels that showed good antibacterial activity

against *E. coli* and *S. aureus* bacteria. Gamma-ray irradiation can be used as a simple method to obtain AgNPs [31]. The exposure of Ag^+ ions to γ radiation in an aqueous medium leads to the formation of Ag^0 in a redox reaction induced by the products of H_2O radiolysis, including hydrogen atom (H) and hydrated electron (e-aq) [31], as indicated in the following reactions.

$$H_2O \rightarrow \text{e-aq, OH, H, } H_3O+, H_2, H_2O_2 \quad (1)$$

$$Ag^+ + e^-_{aq} \rightarrow Ag^0 \quad (2)$$

$$Ag^+ + H^{\cdot} \rightarrow Ag^0 + H^+ \quad (3)$$

In a medium containing a stabilizing agent or in a polymer matrix, the formation of AgNPs occurs [32]. Hence, the gamma radiation was used in this work not only to obtain silver nanoparticles in situ but also because it confers sterilization and cross-linking with the hydrogel in one step at ambient conditions, without the addition of initiators or further controlling. Finally, the work purposes are the development of PVGA/alginate/AgNPs-based hydrogel through PVA acetalization, using gamma radiation for cross-linking, sterilization and incorporation of silver nanoparticles obtainment, including characterizations and evaluation of its biodegradation behavior as a possible wound dressing application material.

Materials

Alginate of low molecular weight from Sigma-Aldrich was used as received. Silver nitrate and PVA (110,000 M_w 99% hydrolyzed) were used as a received. Glyoxylic 50 % in water solution, and sodium hydroxide from Exodo Brazil were used as a received. Hydrochloric acid and acetone 99% from Labsynth Brazil were used as received.

Methods

Irradiation of the blend PVGA–Alginate and $AgNO_3$ salt

PVGA was synthesized following a procedure described in our previous work [21]. A mixture of sodium glyoxylate (SG) and glyoxylic acid (GA) (SG/GA= 0.8 molar ratio adjusted at pH 4 with NaOH) was added to 150 mL of 8% (w/v) PVA water solution (99% hydrolyzed, M_w 110,000) and heating at 75 °C by 2 h in constat stirring. After synthesis, the non-cross-linked polymer was purified by precipitation in acetone, followed by Soxhlet extraction for 48 h, subsequent washing with ice-cold distilled water three times and finally dried in vacuum for 3 days at 50 °C until constant weight [6]. Six formulations of PVGA aqueous solution and sodium alginate (100:0, 90:10, 75:25, 60:40, 50:50 and 40:60) were prepared. The solutions were irradiated at a dose of 30 kGy.

Gel fraction

The obtained PVGA–alginate hydrogel was dried first in an oven at 50 °C for 48 h and weighted (W_i). The dried xerogel samples were put in Soxhlet for 24 h in distilled water as a solvent for removing uncross-linked polymer from the hydrogel. The sample was then dried directly at 50 °C in an oven and weighed again (W_f). The gel fraction (GF%) is calculated by Eq. (4).

$$\mathrm{GF\%} = \frac{W_f}{W_i} \times 100 \tag{4}$$

Swelling behavior

Just after radiation process (not dry conditions), rectangle samples of PAlg-75:25 of 2 cm × 2 cm length and 3 mm of thickness were immersed in a glass container with excess distilled water or buffer physiological saline solution with ionic strength equal to 1 (approximately 10 mL) at 37 °C and then weighted at specific time interval. The attached water on the surface of hydrogels was blotted with filter paper. Three replicates were performed for each composition. The test was done 24 h. The swelling degree was determined by Eq. 5.

$$\mathrm{Swelling\%} = \frac{W_\mathrm{s} - W_\mathrm{ai}}{W_\mathrm{ai}} \times 100 \tag{5}$$

where W_ai = weight of polymer after irradiation; W_s = weight of a swollen polymer.

Measurements

FTIR-ATR spectra were recorded on previously dried samples using spectrometer Nicolet 6700 spectrometer. MCT detector, PerkinElmer Spectrum 100 Instruments, USA, was fitted with a Universal ATR sampling accessory (DiCompTM crystal, which is composed of a diamond ATR with a zinc selenide focusing element in direct contact with the diamond from 400 to 4000 cm^{-1}). Thermogravimetric analysis (TGA) of samples was carried out using Mettler-Toledo TGA/SDTA 581 thermobalance in nitrogen atmosphere from 25 to 600 °C at heating rate of 10 °C min^{-1}. Silver nanoparticles were characterized directly on the UV–visible Spectroscopy Molecular Devices SpectraMax M I3 in a wavelength range between 300 and 600 nm. Field Emission Gun Scanning Electron Microscopy (SEM-FEG), the JOEL 2100, was used to observe the AgNPs in the hydrogel; samples were lyophilized before test.

Cytotoxicity assay

Cytotoxicity assay was performed using NCTC Clone 929 cells exposed to the diluted samples extracts, without and with AgNPs, and the pure PVGA hydrogel. Cell viability

was determined on an Elisa reader at 540 nm with a reference filter of 620 nm. Positive control extracts of LBD and polyethylene rubber as negative control were also placed.

Soil biodegradation test

The specimen dimensions were approximately 5.0×5.0×3 mm (width×length×thickness) by triplicate. The specimens were embedded in circular pots (15 cm of diameter), containing 20 cm of plant soil at pH 6.0. The samples were previously dried in the oven at 32 °C for 2 days and weighed. The composting process preceded with an initial increase in temperature up to 35 °C during all experiment. During the composting process, distilled water was added to maintain 50% moisture content on a total weight basis. The procedure was followed 12 days. Weight loss was determined every 15 days, then, the samples were dug up, brushed, cleaned and dried in an oven-dried at 32 °C ± 5 °C for 2 days, until no changes in weight. After that, all samples were placed in a desiccator for 1 h and allowed to cool and finally, dried films were weighed. The reduction in the mass percentage of the samples due to the degradation process is calculated by Eq. 6, but in this case, W_d and W_s are the weight of the sample before and after degradation, respectively.

$$\text{Soil biodegradation}\% = \frac{W_d - W_s}{W_d} \times 100 \tag{6}$$

Results and discussion

Gel fraction (GF)

The gel fraction (GF) of 100:0, 90:10, 75:25, 60:40, 50:50, and 40:60 PVGA/Alg were determined. To GF test, samples without Ag salt were evaluated (Fig. 1).

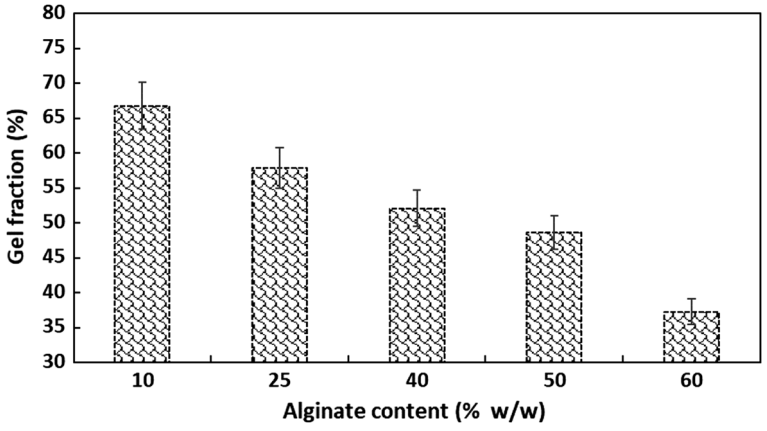

Fig. 1 Gel fraction % versus alginate content. Samples blended with PVGA without silver nitrate

Visually, the sample 40:60 was very sticky to handle. The 75:25 and 60:40 samples reticulated perfectly, but the 60:40 sample was brittle. The samples with 100:0, 90:10 also reticulated perfectly. Figure 1 shows the GF% for all samples versus alginate content. The gel part decreases when Alg content increases. After irradiation, alginate was not cross-linked. Due to easy hand manipulation and almost 83% of PVGA was cross-linked, the formulation of PVGA–alginate 75:25 (PAlg-75:25) was chosen to be irradiated with 32 ppm of $AgNO_3$ salt. Assuming that 100% of $AgNO_3$ convert to AgNPs, 30 ppm of AgNPs would be enough to obtain a bactericidal effect according to Qing and co-workers [33, 34].

FTIR analysis

Figure 2 shows the IR spectra of hydrogel components. The bands of pristine alginate were associated with the stretching OH vibrations in 3250 cm^{-1} and 1315 cm^{-1}, asymmetric and symmetrical vibration of the carbonyl group (COO^-) in 1595 cm^{-1} and 1406 cm^{-1}, a band at around 2930 cm^{-1} of the stretching vibrations of aliphatic C–H and the bands corresponding to C–C–C and C–O–C of pyranic bond in 1082 cm^{-1} and 1026 cm^{-1} respectively [35]. According to our previous work, irradiated PVGA shows a band at 1612 cm^{-1} that corresponds to carboxylic (COO^-) pending on the cyclic acetal group. At 3250 cm^{-1} and 1425 cm^{-1} is located the characteristic OH from non-reacted PVA alcohol and at 2935 cm^{-1} is located the stretching band of CH_2 and CH_3 signals. In the spectrum of the sample PAlg-75:25 (after irradiation), the stretching bands of the O–H and (COO^-) groups from calcium alginate are partially overlapped with the bands of the same groups of the PVGA, although, a little displacement is present (~2%), in the (COO^-) bands of PVGA

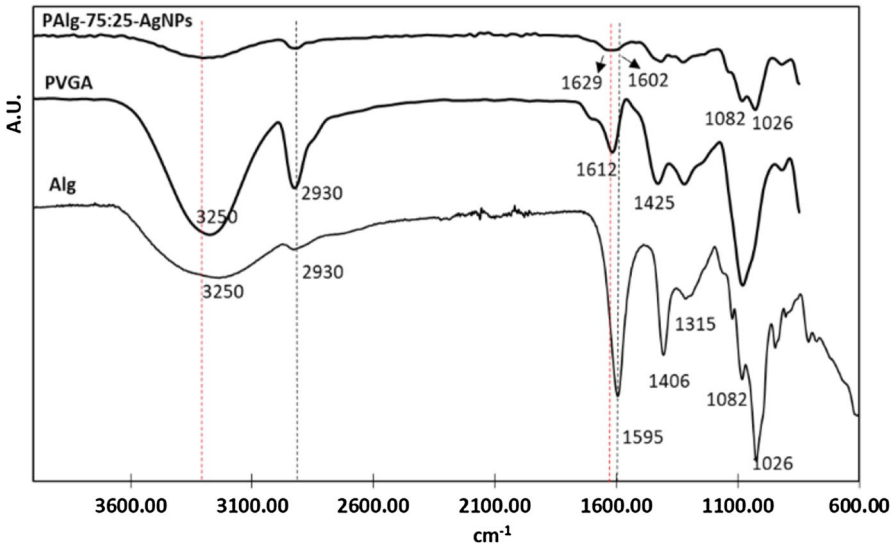

Fig. 2 FTIR analysis of pure Alg, pure PVGA and PAlg-75:25- AgNPs after irradiation

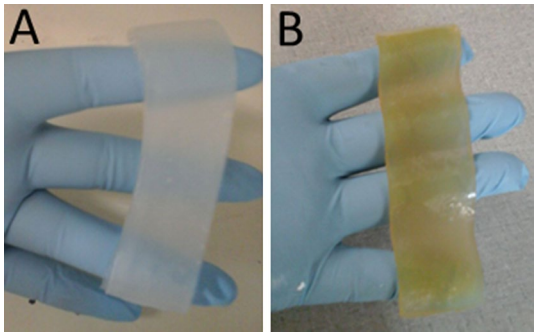

Fig. 3 **a** PAlg-75:25 and **b** PAlg-75:25-AgNPs after irradiation

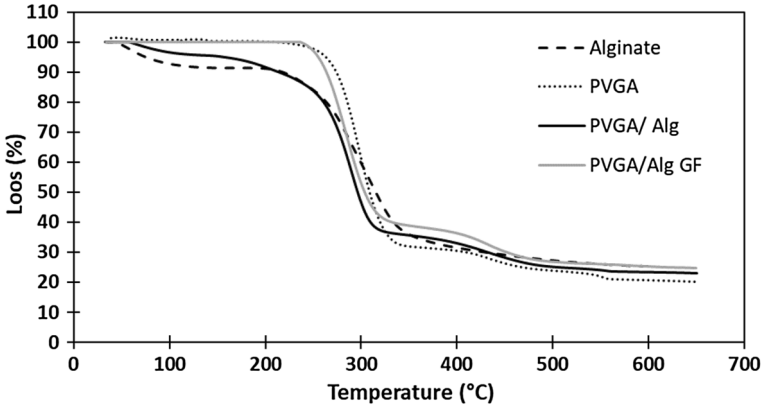

Fig. 4 TGA profile of pure alginate, pure PVGA, PAlg-75:25 and its gel fraction

showed at higher wavelength in 1629 cm^{-1}. The bands C–C–C (1082 cm^{-1}) and C–O–C (1026 cm^{-1}) corresponding to the alginate glycosidic bond are present too.

Figure 3a, b shows the (PAlg-75:25) irradiated with and without $AgNO_3$ salt. After the gamma irradiation, the yellow-colored colloids were obtained, which is characteristic of Ag nanoparticles. These colloids are transparent and stable for an extended time. This indicates that there is no agglomeration of AgNPs.

Thermal analysis

TGA thermogram shows the weight loss of Alg, PVGA, PAlg-75:25 and its gel fraction (Fig. 4). Thermogravimetric behavior of calcium alginate and other polysaccharides begins with dehydration [36], after that continues the dehydration of saccharide rings at 110 °C and breaking of C–O–C bonds at 220 °C. Finally the main chain degradation starts at 528 °C with subsequent formation CO, CO_2 CH_4 and H_2O [37–40]. PVGA exhibited three different temperature degradation changes. The first one at 280 °C occurs due to the decomposition of alcohol groups present in

pendant groups in the main chain. At 420 °C decomposition of CH_2 group starts followed by decomposition of acetal cyclic groups present in the main chain at 550 °C.

The TGA decomposition profile for the PVGA–alginate hydrogel is noticeably different than that observed for the pure PVGA (T10% are 60 °C lower than pure PVGA pure hydrogel) and appears to have features found in both alginate and PVGA data. These observations prove the incorporation of the alginate in the formula besides suggesting its small degradation. The gray line in the thermogram represents the degradation pattern of the gel fraction of PAlg-75:25 sample, which has shown a typical PVGA polymer behavior, which evidences that the alginate does not cross-link [21]. Possibly the alginate chains were curling in the chains of the cross-linked PVGA forming a pseudo-IPN.

Characterization of AgNPs by UV–Vis spectroscopy

Figure 5 shows UV–visible absorption spectra of pure PAlg-75:25 and PAlg-75:25/AgNPs nanocomposites from 3 to 42 days after irradiation; the irradiation process was able to reduce ionic silver in situ, which indicates the presence of surface plasmon resonance (SPR) bands, with the characteristic maximum absorption at about 410 nm. Regarding the absorption spectrum of the pure PVGA–Alg, a nearly zero absorption as well as un-radiated Ag salt solution can be seen. Three days after exposure to gamma radiation, AgNPs were stable, whose stability was lost over time

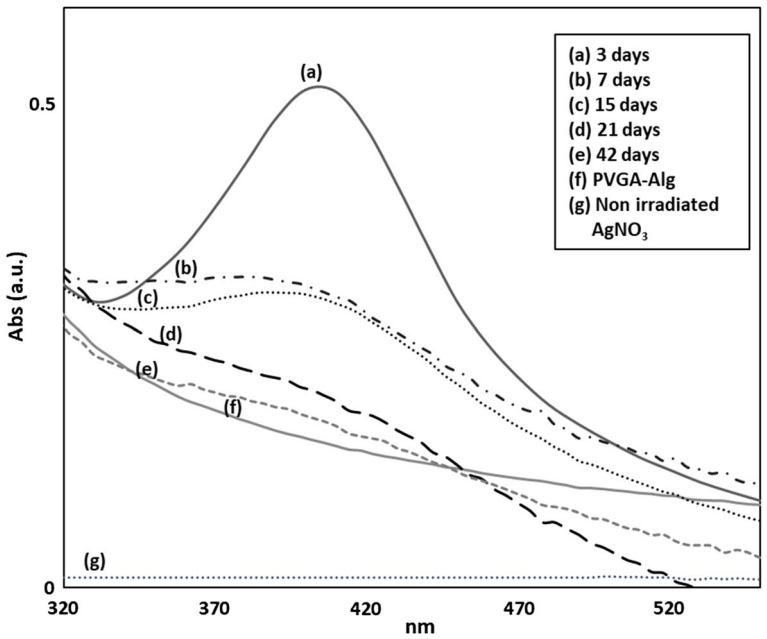

Fig. 5 UV–visible absorption spectra of pure PAlg-75:25 and PAlg-75:25/AgNPs nanocomposites from 3 to 42 days after irradiation

and after the exposition to the air. Initially, to prevent clusters collision and their growth into bigger nanoparticles, the polymer molecules with functional groups that have an excellent affinity for metals were added. In the case of PVGA and Alg, the COOH and hydroxyl(OH)groups interact with the atoms on the surface of metal nanoparticles and thus stabilize them, preventing their agglomeration and further growth (Scheme 1). After the gamma irradiation, yellow-colored PAlg-75:25/AgNPs hydrogels were obtained, which is characteristic of Ag nanoparticles. These colloids are yellow and stable for almost 15 days in air. After this time, the agglomeration of AgNPs was observed, and the hydrogel losses yellow color at starting just after irradiation.

Characterization SEM/FEG of PVGA–Alg/AgNPs

Figure 6 displays microscopy of the PAlg-75:25/AgNPs hydrogel, analyzed by SEM/FEG. Figure 6a shows the cross-sectional fracture surface; the fracture has a hydrogel appearance, but there was no possibility to observe the AgNPs, because they are embedded into the bulk. Samples with 3 and 21 days of exposition to

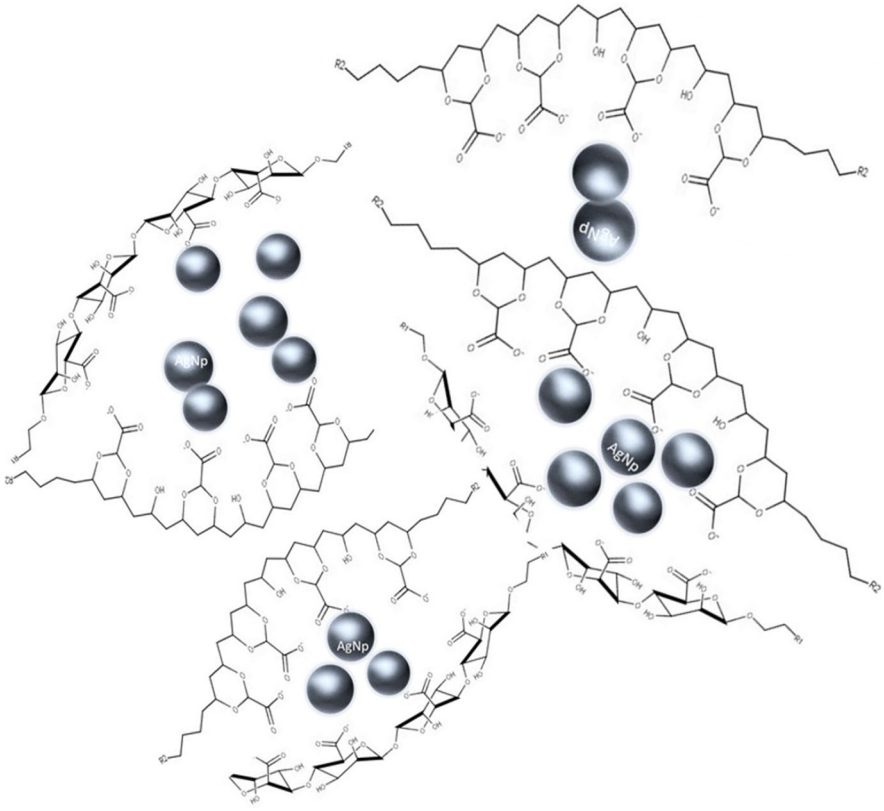

Scheme 1 Representation of AgNPs stabilization by the COOH groups from PVGA and Alg

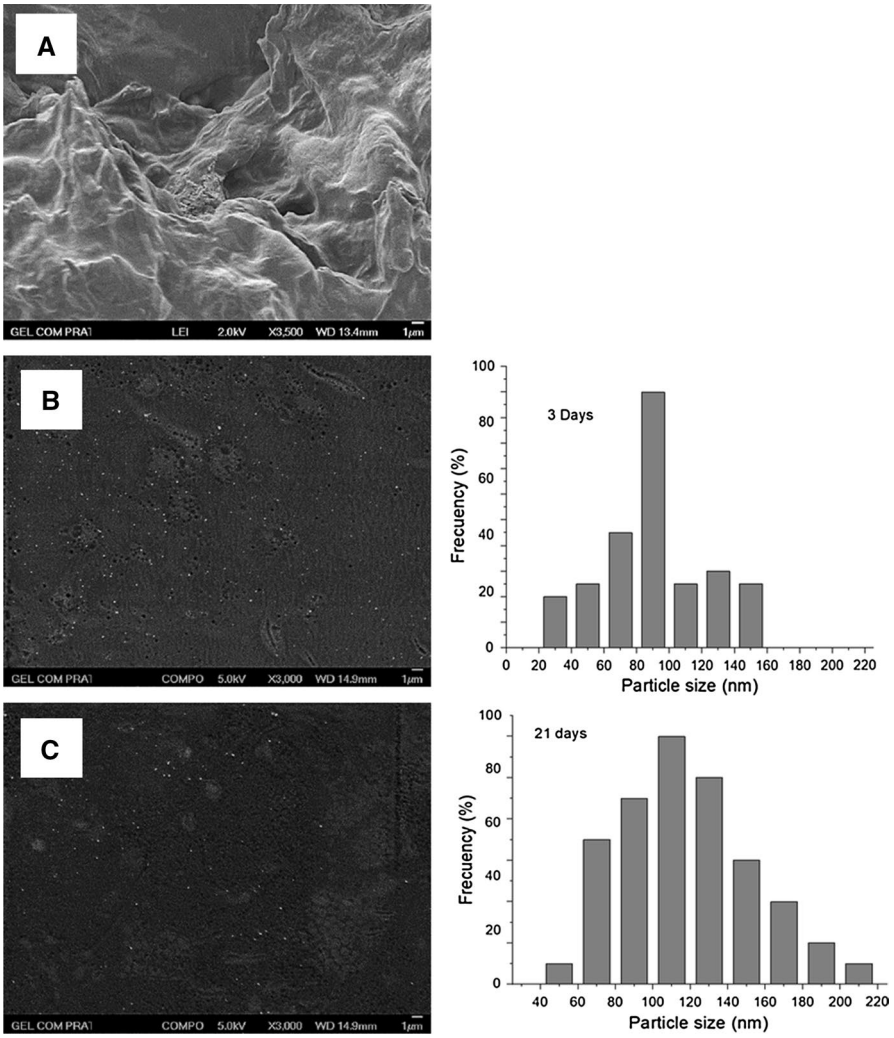

Fig. 6 Characterization by SEM of **a** PAlg-75:25/AgNPs, **b** SEM-FEG PAlg-75:25/AgNPs after 3 days of exposure to air and **c** SEM-FEG PAlg-75:25/AgNPs after 21 days of exposure to air

air were analyzed by SEM-FEG, and it was possible to evidence the presence of AgNPs. ImageJ software was used to build the particle size distribution histograms. The distribution histograms were homogeneous at first 3 days after irradiation as shown in Fig. 6b. The histogram displays AgNPs sizes average of 90 nm which is also favorable because higher bactericidal efficiency is achieved at shorter particle sizes; an inverse correlation between nanoparticle size and antimicrobial activity has been demonstrated [41]. Nevertheless, 21 days after irradiation and exposure to air, histograms built from ImageJ show a little increment in the size of AgNPs and a reduction in quantity because of the possibility of the agglomeration and sizes

increase of AgNPs (Fig. 6c); this fact then can explain the decrease in absorbance after 21 days of exposure to the air.

Swelling analysis

After 24 h of irradiation, the hydrogels were cut into identical pieces of 2 cm × 2 cm, weighed and submerged in 100 mL of buffer solutions (pH 3, 7 and 10), distilled water and saline solution by triplicate.

Figure 7 shows the swelling degree in pure water, saline solution and buffer solutions of pH 3, 7 and 1. Swelling in pure water displays the highest swelling with 5.6 times after irradiation (not dry), followed by a saline solution with 2.6 times. In this case, free Na^+ Cl^- remains inside the gel to neutralize the charges on the network chains. The driving force of the swelling process is the presence of mobile osmotically active counterions. When salt is added to the system, ions diffuse from the solution into the network. The overall concentration of mobile ions in the gel is still higher than before, but the difference between ion concentrations inside and outside is reduced.

Consequently, the driving force of swelling decreases gradually with increasing salt concentration [42, 43]. At pH 3 and 7, the carboxylic acid group is protonated COOH, there are not repulse charges, and the hydrogel is collapsed. When pH decreases to acidic values, the COOH group was totally protonated and less quantity of water is attracted to the bulk, and then, the swelling decreases. On the contrary, at basic conditions at pH 10, the swelling increases because the electric charge in COO^- attracts more water molecules to the inner bulk of hydrogel. These tests show the efficacy of these materials in an application of absorbent material to high exudate grade (venous ulcer, for example) where the exudate

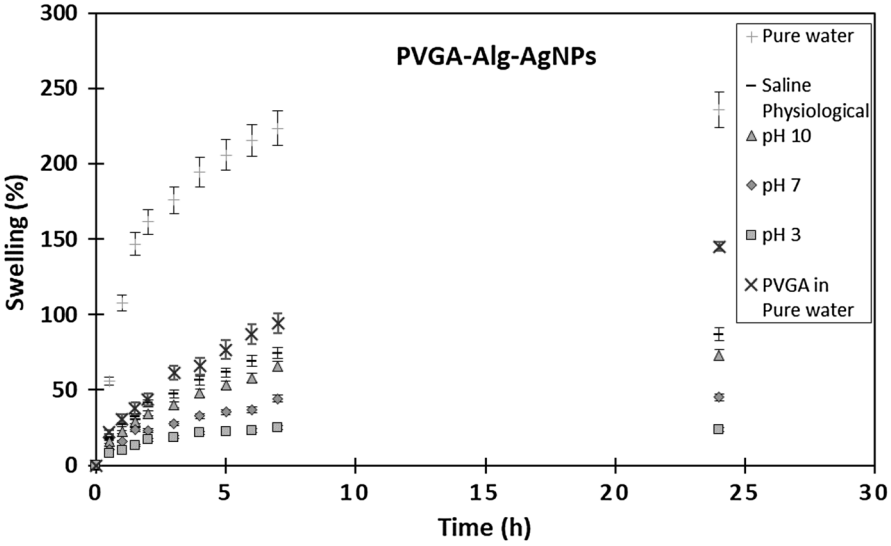

Fig. 7 Swelling behavior of PAlg-75:25/AgNPs in different mediums

contains a wide variety of salts and proteins that may decrease the absorption efficiency of the dressing.

Biodegradation

This material was designed to assist in the treatment of high exudate wounds in hospitals. Then, it is essential that it also responds to the needs of the environment. The reason to measure biodegradation degree of the material in a ground test is that many of the solid wastes are discarded and confined in soil or landfills [44, 45].

An initial visual characterization of samples PAlg-75:25/AgNPs displays samples grayish colored; it was found that the degradation degree rises with increasing the biodegradation time. The surface of the samples turns irregular and presents cracks over time an associate at the weight loss.

Weight loss percentage was measured gravimetrically, and the result is shown in Fig. 8. In the first 15 days, degradation percentage was 26% which probably corresponds mainly to the biodegradation of the alginate, for two reasons: (i) the hydrolytic susceptibility of glycosidic bond; (ii) the poor or null cross-linking of alginate backbone, producing faster biodegradation. In the interval of 30–105 days, the material was gradually degrading, and then, at 120 days, the accelerating process occurs. At this point, the texture of the material is brittle. The maximum degree of biodegradation reached was 37% in the first 4 months. However, the trend indicates that at a given moment, the material must disintegrate almost wholly.

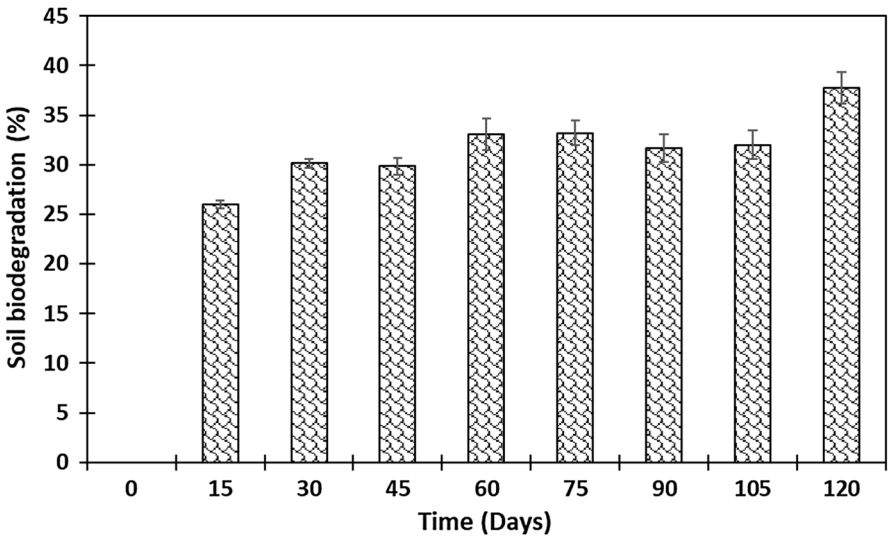

Fig. 8 Soil biodegradation % versus time of PAlg-75:25/AgNPs, measurement by weight lose

FTIR spectra of PAlg-75:25/AgNPs after composting

Changes in chemical structure upon biodegradation were evaluated through FTIR spectroscopy. Figure 9 displays the FTIR spectra of PAlg-75:25/AgNPs before and after 15, 60 and 120 days of composting. At 0 days, as mentioned above the stretching bands of the O–H groups are represented at 3250 cm^{-1}. The band at 2939 cm^{-1} is the characteristic band of asymmetric C-H stretch of the alkyl groups. The bands at 1629 cm^{-1} and 1602 cm^{-1} were attributed to the stretching vibrations of C=O of carbonyl acid of PVGA and PVGA and alginate, respectively, including a displacement (~ 2%), the bands C–C–C (1082 cm^{-1}) and C–O–C (1026 cm^{-1}) corresponding to the alginate glycosidic bond. At first 15 days after composting, the band C–O–C corresponding to the glycosidic bond of alginate decreased substantially, indicating the rupture of the main chain. The spectrum also shows at first 15 days decrease in the intensity of the asymmetric vibration C=O band at 1602 cm^{-1}. At the next 60 days after composting, the band C=O at 1602 cm^{-1} from alginate almost disappeared and the band of the same group but from PVGA in 1629 cm^{-1} begins to decrease, suggesting that the decarboxylation of PVGA starts and decarboxylation of alginate has been completed. After 3 months, the spectrum was very similar to pure PVA and the band of asymmetric C-H stretch of the alkyl groups represented in 2939 cm^{-1} decreased its intensity due to the weight loss of main functional groups and the backbone degradation.

TGA characterization of PAlg-75:25/AgNPs after composting

Complementary thermal characterization of the sample at 0, 60, 120 days after composting is shown in Fig. 10. Before composting, thermal degradation is performed in three steps: first, dehydration alginate; second decarboxylation of both PVGA and alginate; and third, degradation of the main backbone. At 60 and more remarkable at

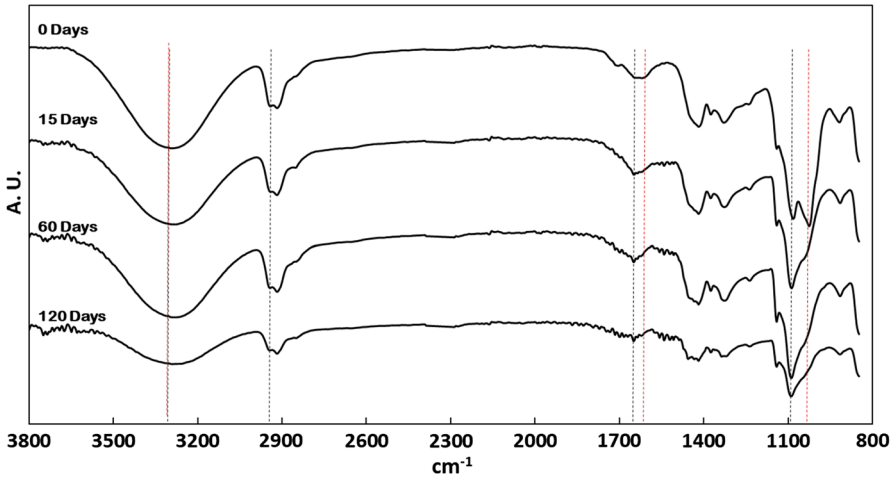

Fig. 9 Evolution of FTIR spectra of PAlg-75:25/AgNPs after composting

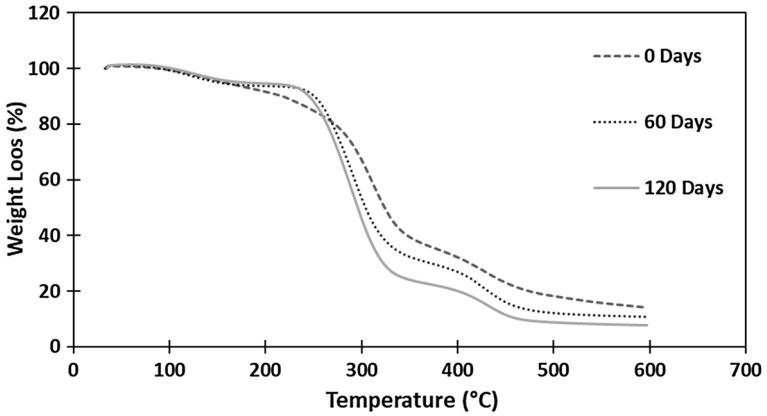

Fig. 10 Evolution of TGA characterization of PAlg-75:25/AgNPs after composting

120 days, the first and second steps changed its thermal behavior due to the chemical composition of samples that have been changing. After 120 days, the thermal stability of the main backbone decreased because of biodegradation process, and when compared with pure PVGA, we can see that first step (dehydration) persisted which does not refer to alginate but does to PVA that is an intermediate of PVGA biodegradation process which is according to the FTIR above.

According to the results presented above, we proposed a mechanism of biodegradation as follows.

According to our previous work, PVGA is a functionalized PVA (30% of modification) [21]. The proposed mechanism was based on TGA and FTIR data in the first 120 days of composting (Scheme 2). In the literature, there are several studies of biodegradation of alginate and PVA [46, 47], but this work encloses the biodegradation on the mixture of modified PVA and alginate.

In the first 15 days, FTIR shows decrease in the intensity of the C–O–C band corresponding to the glycosidic bond of alginate indicating the rupture of the main chain. Also, a decrease in the intensity of the asymmetric vibration C=O band at 1602 cm^{-1} corresponding to the carbonyl group from alginate suggests the degradation of the functionalities of its pyran group. At the next 60 days after composting, the band C=O at 1602 cm^{-1} from alginate almost disappeared and the band of C=O at 1629 cm^{-1} from PVGA in 1629 starts to decrease, suggesting the decarboxylation of PVGA. At 60 days, alginate loses their characteristic C=O bond evidenced by the fading of the band in 1602 cm^{-1} and probably follows the mechanisms proposed by Jeon [48] by pyran ring rupture. At 60 days of composting the loss of OH groups of alginate is evident, suggesting that the pyran group was not degraded but at 120 days, the thermal behavior of alginate is similar than PVGA, although the stability of main backbone decreased when compared with pristine PVGA. At the same 120 days, it is possible to see the first step (alcohol group degradation) which does not refer to alginate but does to PVA (OH groups) that is an intermediate of PVGA in the biodegradation process which is according to FTIR. After 3 months, the spectrum was very similar to pure PVA and the band of asymmetric C–H stretch of the

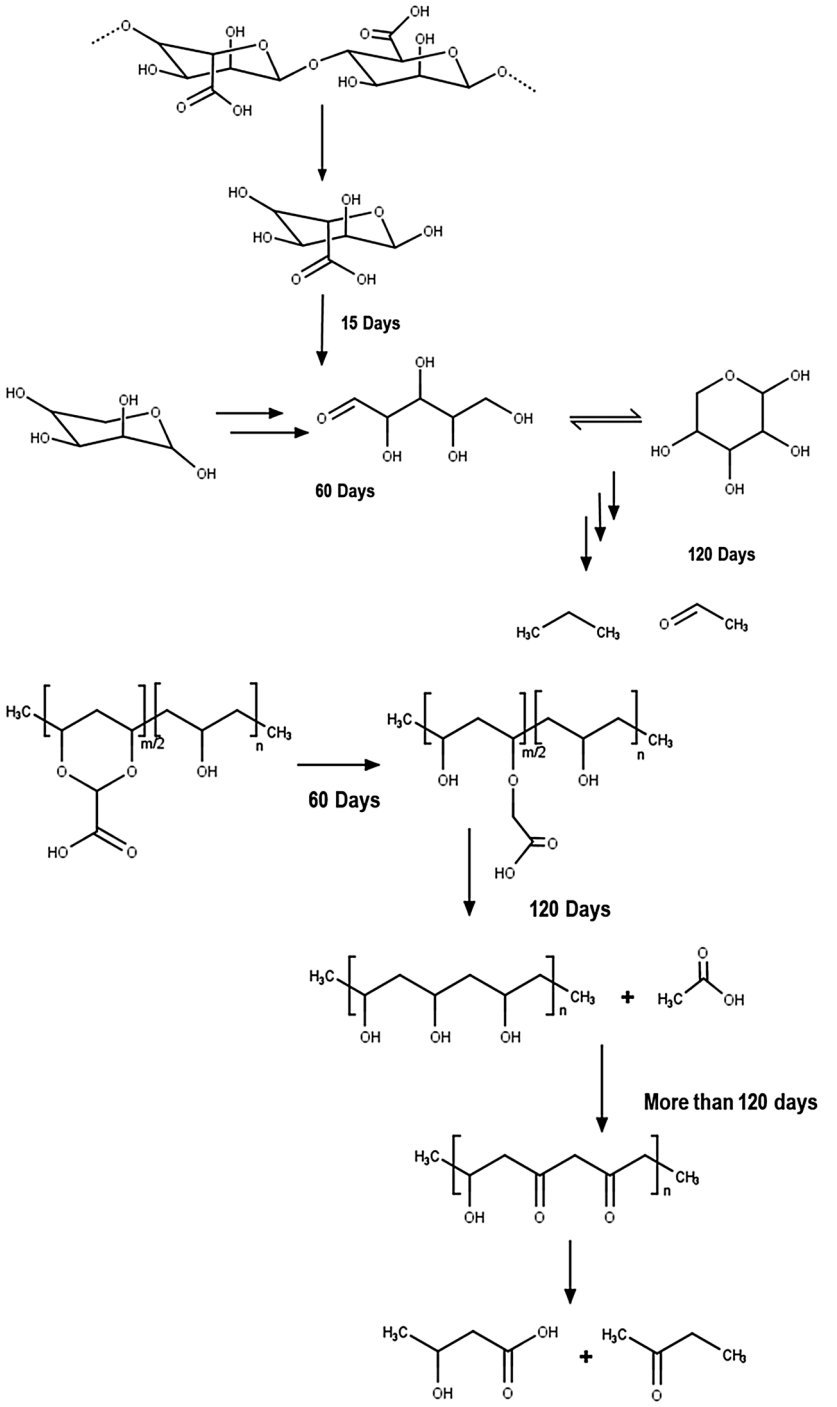

Scheme 2 Proposed biodegradation mechanism of PAlg-75:25/AgNPs

alkyl groups represented in 2939 cm^{-1} decreased its intensity due to the weight loss of the CH_2–CH_3 of acetal groups and the backbone degradation [49]. At 120 days, the mechanism follows the route proposed by Jayasekara [50] to composting biodegradation of PVA.

In other words, the proposed mechanism is based on results of FTIR and TGA data that explains the first 120 days of composting; after that and according to the FTIR results, the biodegradation mechanism follows the route of PVA. This asseveration can be based on the studies made by Jayasekara [51], where the biodegradation of different blends of modified starch and PVA was studied, and compost was evaluated for 45 days. The partly degraded films were recovered and analyzed by SEM, x-ray diffraction and FTIR techniques. The authors found that the modified films also degraded, leaving the PVA component behind. It was also demonstrated (spectroscopically) that the chitosan coating also wholly degraded. In complementation, Pseudomonas species present in soil are so crucial in the cleavage mechanism for degradation of PVGA and PVA [52, 53]. According to the literature under this condition (composting), a possible way of biodegradation of PVA is following the formation of β-diketone by oxidation of OH group and consecutively formation of methyl ketone and a carboxylic acid from the longer and the shorter segment catalyzed by Pseudomonas present in composting [54].

Cellular viability of PAlg-75:25/AgNPs and its components

The results show that cell viability for all samples was 100%, indicating that each element that makes up the dressing is not cytotoxic. Samples have the same behavior as a positive control, and therefore, the sample can be used as a biomaterial without causing injury to the surrounding cells (Fig. 11).

Conclusions

In this study, PVA-Alg/AgNPs hydrogels were prepared by radiation technology for usage in wound dressing applications. Gamma radiation is found suitable as a technique for the incorporation of AgNPs in situ in cross-linked PVGA polymer matrix. Formulation of PAlg-75:25/AgNPs hydrogel, which is absorbent and non-cytotoxic, is easy to be biodegraded in soil because of the mixture of a natural and synthetic biodegradable polymer. The hydrogels have suitable properties for use as absorbent material dressings: pH sensitivity, swelling and non-cytotoxicity. The results of the AgNPs stability study indicated that PAlg-75:25/AgNPs hydrogels are stable for 6 days when exposed to air. After this period, the particles become too aggregate. PVA-Alg/AgNPs hydrogels prepared by radiation have good approach for wound dressing application.

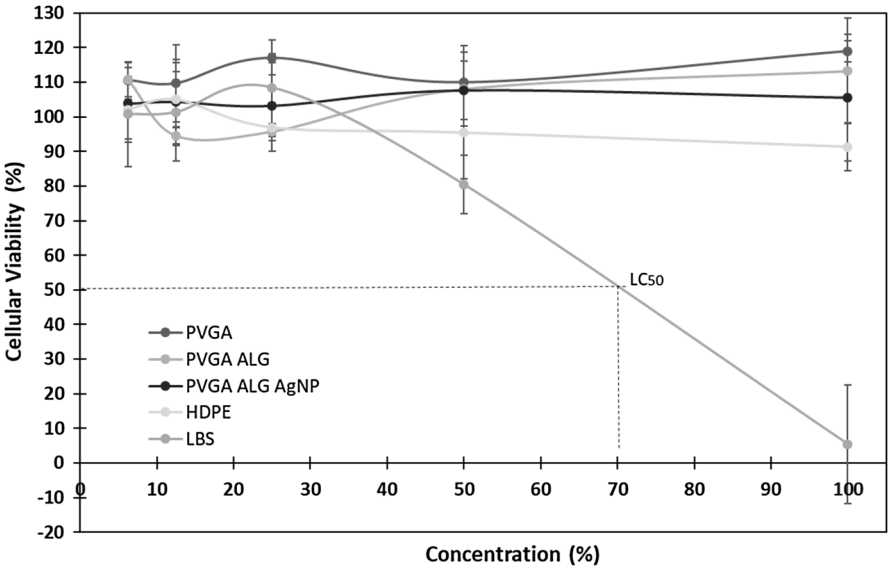

Fig. 11 Cell viability curve in the cytotoxicity assay by the PAlg-75:25/AgNPs

Funding We also thank M.Sc. Pablo A. S. Vásquez, Center for Radiation Technology (CTR-IPEN-SP), for irradiation support; Microscopy and Microanalysis Laboratory (CCTM-IPEN-SP) and project CONACYT 296395 for partial support.

References

1. Peppas NA, Slaughter BV, Kanzelberger MA (2012) Hydrogels. In: Polymer science: a comprehensive reference, Elsiever (ed), vol 9. pp 385–395. https://doi.org/10.1016/b978-0-444-53349-4.00226-0
2. Lima-Tenório MK, Tenório-Neto ET, Guilherme MR, Garcia Francielle P, Nakamura CV, Pineda EAG, Rubira AF (2015) Water transport properties through starch-based hydrogel nanocomposites responding to both pH and a remote magnetic field. Chem Eng J 259:620–629. https://doi.org/10.1016/j.cej.2014.08.045
3. Kamath KR, Park K (1993) Biodegradable hydrogels in drug delivery. Adv Drug Deliv Rev 11:59–84. https://doi.org/10.1016/0169-409X(93)90027-2
4. White R, Cutting KF (2006) Modern exudates management: a review of wound treatments. World Wide Wounds 1.0. http://www.worldwidewounds.com/2006/september/White/Modern-Exudate-Mgt.html
5. Kamoun EA, El-Refaie KS, Tamer TM, El-Meligy MA, Eldin MSM (2015) Poly (vinylalcohol)-alginate physically cross-linked hydrogel membranes for wound dressing applications: characterization and bio-evaluation. Arab J Chem 8:38–47. https://doi.org/10.1016/j.arabjc.2013.12.003
6. Salehpour S, Jonoobi M, Ahmadzadeh M, Siracusa V, Rafieian F, Oksman K (2018) Biodegradation and ecotoxicological impact of cellulose nanocomposites in municipal solid waste composting. Int J Biol Macromol 111:264–270. https://doi.org/10.1016/j.ijbiomac.2018.01.027

7. Chiellini E, Solaro R (1996) Biodegradable polymeric materials. Adv Mater 8:305–313. https://doi.org/10.1002/adma.19960080406
8. Bhattacharya A (2000) Radiation and industrial polymers. Prog Polym Sci 25:371–401. https://doi.org/10.1016/S0079-6700(00)00009-5
9. Immirzi B, Santagata G, Vox G, Schettini E (2009) Preparation, characterization and field-testing of a biodegradable sodium alginate-based spray mulch. Biosyst Eng 102:461–472. https://doi.org/10.1016/j.biosystemseng.2008.12.008
10. Bastioli C (2005) Editor handbook of biodegradable polymers rapra technology limited. Shrewsbury, U.K. Rapra Technology
11. Tudorachi N, Cascaval CN, Rusu M, Pruteanu M (2000) Testing of polyvinyl alcohol and starch mixtures as biodegradable polymeric materials. Polym Test 19:785–799. https://doi.org/10.1016/S0142-9418(99)00049-5
12. Hebeish A, Hashem M, El-Hady MM, Sharaf S (2013) Development of CMC hydrogels loaded with silver nano-particles for medical applications. Carbohydr Polym 92:407–413. https://doi.org/10.1016/j.carbpol.2012.08.094
13. Jawaid M, Abdul Khalil HPS (2011) Cellulosic/synthetic fibre reinforced polymer hybrid composites: a review. Carbohyd Polym 86:1–18
14. Ikejima T, Inoue Y (2000) Crystallization behavior and environmental biodegradability of the blend films of poly(3-hydroxybutyric acid) with chitin and chitosan. Carbohydr Polym 41:351–356. https://doi.org/10.1016/S0144-8617(99)00105-8
15. Roy N, Saha N, Kitano T, Saha P (2012) Biodegradation of PVP-CMC hydrogel film: a useful food packaging material. Carbohydr Polym 89:346–353. https://doi.org/10.1016/j.carbpol.2012.03.008
16. Ying-Ning P, Swee-Yong C, Chee-Onn L, Yok-Lan T (2011) Thermal and microbial degradation of alginate-based superabsorbent polymer. Polym Degrad Stab 96:1653–1661. https://doi.org/10.1016/j.polymdegradstab.2011.06.010
17. Yoo-Joo K, Kee-Jong Y, Sohk-Won K (2000) Preparation and properties of alginate superabsorbent filament fibers crosslinked with glutaraldehyde. J Appl Polym Sci 78:1797–1804. https://doi.org/10.1002/1097-4628(20001205)78:10%3c1797:aid-app110%3e3.0.co;2-m
18. Kamoun EA, El-RS Kenawy, Chen X (2017) A review on polymeric hydrogel membranes for wound dressing applications: PVA-based hydrogel dressings. J Adv Res 3:217–233. https://doi.org/10.1016/j.jare.2017.01.005
19. Shalumon KT, Anulekha KH, Sreeja VN, Nair SV, Chennazhi KP, Jayakumar R (2011) Sodium alginate/poly(vinyl alcohol)/nano ZnO composite nanofibers for antibacterial wound dressings. Int J Biol Macromol 49:247–254. https://doi.org/10.1016/j.ijbiomac.2011.04.005
20. Kim JO, Park JK, Kim JH, Jin SG, Yong CS, Li DX, Choi JY, Woo JS, Yoo BK, Lyoo WS, Kim JA, Choi HG (2008) Development of polyvinyl alcohol–sodium alginate gel-matrix-based wound dressing system containing nitrofurazone. Int J Pharm 359:79–86. https://doi.org/10.1016/j.ijpharm.2008.03.021
21. Estrada Villegas GM, Morselli GR, González-Pérez G, Lugão AB (2018) Enhancement swelling properties of PVGA hydrogel by alternative radiation cross-linking route. Radiat Phys Chem 153:44–50. https://doi.org/10.1016/j.radphyschem.2018.08.038
22. Thoniyot P, Tan MJ, Karim AA, Young DJ, Loh XJ (2015) Nanoparticle-hydrogel composites: concept, design, and applications of these promising, multi-functional materials. Adv Sci 2:1400010. https://doi.org/10.1002/advs.201400010
23. Lyutakov O, Goncharova I, Rimpelova S, Kolarova K, Svanda J, Svorcik V (2015) Silver release and antimicrobial properties of PMMA films doped with silver ions, nano-particles and complexes. Adv Mater Sci Eng C 49:534–540. https://doi.org/10.1016/j.msec.2015.01.022
24. Rai M, Yadav A, Gade A (2009) Silver nanoparticles as a new generation of antimicrobials. Biotechnol Adv 27:76–83. https://doi.org/10.1016/j.biotechadv.2008.09.002
25. Fu LH, Gao QL, Qi C, Ma MG, Li JF (2018) Microwave-hydrothermal rapid synthesis of cellulose/Ag nanocomposites and their antibacterial activity. Nanomaterials 27:1–13. https://doi.org/10.3390/nano8120978
26. Chandran S, Ravichandran V, Chandran S, Chemmanda J, Chandarshekar B (2016) Biosynthesis of PVA encapsulated silver nanoparticles. J Appl Res Technol 14:319–324. https://doi.org/10.1016/j.jart.2016.07.001
27. Becaro AA, Jonsson CM, Puti FC, Siqueira MC, Mattoso LHC, Correa DS, Ferreira MD (2015) Toxicity of PVA-stabilized silver nanoparticles to algae and microcrustaceans. Environ Nanotechnol Monit Manag 3:22–29. https://doi.org/10.1016/j.enmm.2014.11.002

28. Eghbalifam N, Frounchi M, Dadbin S (2015) Antibacterial silver nanoparticles in polyvinyl alcohol/sodium alginate blend produced by gamma irradiation. Int J Biol Macromol 80:170–176. https://doi.org/10.1016/j.ijbiomac.2015.06.042
29. El-Shamy AG, Attia WM, Kader KMA (2017) Enhancement of the conductivity and dielectric properties of PVA/Ag nanocomposite films using γ irradiation. Mater Chem Phys 191:225–229. https://doi.org/10.1016/j.matchemphys.2017.01.026
30. Swaroop K, Francis S, Somashekarappa HM (2016) Gamma irradiation synthesis of Ag/PVA hydrogels and its antibacterial activity. Mater Today Proc 3:1792–1798. https://doi.org/10.1016/j.matpr.2016.04.076
31. Chen P, Song L, Liu Y, Fang Y (2007) Synthesis of silver nanoparticles by γ -ray irradiation in acetic water solution containing chitosan. Radiat Phys Chem 76:1165–1168. https://doi.org/10.1016/j.radphyschem.2006.11.012
32. Sedlacek O, Kucka J, Monnery BD, Slouf M, Vetrik M, Hoogenboom R, Hruby M (2017) The effect of ionizing radiation on biocompatible polymers: from sterilization to radiolysis and hydrogel formation. Polym Degrad Stab 137:1–10. https://doi.org/10.1016/j.polymdegradstab.2017.01.005
33. Qing Y, Cheng L, Li R, Liu G, Zhang Y, Tang X, Wang J, Liu H, Qin Y (2018) Potential antibacterial mechanism of silver nanoparticles and the optimization of orthopedic implants by advanced modification technologies. Int J Nanomed 13:3311–3327. https://doi.org/10.2147/IJN.S165125
34. Malkar VV, Mukherjee T, Kapoor S (2014) Synthesis of silver nanoparticles in aqueous aminopolycarboxylic acid solutions via γ-irradiation and hydrogen reduction. Mater Sci Eng C 44:87–91. https://doi.org/10.1016/j.msec.2014.08.002
35. Patel GM, Patel CP, Trivedi HC (1999) Ceric-induced grafting of methyl acrylate onto sodium salt of partially carboxymethylated sodium alginate. Eur Polym J 35:201–208. https://doi.org/10.1016/S0014-3057(98)00123-2
36. Adzmi F, Meon S, Hanafi-Musa M, Azah-Yusuf N (2012) Preparation, characterization and viability of encapsulated Trichoderma harzianum UPM40 in alginate-montmorillonite clay. J Microencapsul 29:205–210. https://doi.org/10.3109/02652048.2012.659286
37. Sreedhar B, Sairam M, Chattopadhyay DK, Syamala Rathnam PA, Mohan Rao DV (2005) Thermal, mechanical, and surface characterization of starch–poly(vinyl alcohol) blends and borax-crosslinked films. J Appl Polym Sci 96:1313–1322. https://doi.org/10.1002/app.21439
38. Mohsin M, Hossin A, Haik Y (2011) Thermal and mechanical properties of poly(vinyl alcohol) plasticized with glycerol. J Appl Polym Sci 22:3102–3109. https://doi.org/10.1002/app.34229
39. Laurienzo P, Malinconico M, Motta A, Vicinanza A (2005) Synthesis and characterization of a novel alginate-poly(ethylene glycol) graft copolymer. Carbohyd Polym 62:274–282. https://doi.org/10.1016/j.carbpol.2005.08.005
40. Eldin MSM, Soliman EA, Elzatahry AAF, Elaassar MR, Elkady MF, Rahman AMA, Yossef ME, Eweida BY (2012) Preparation and characterization of imino diacetic acid functionalized alginate beads for removal of contaminants from waste water: I. methylene blue cationic dye model. Desalin Water Treat 40:15–23. https://doi.org/10.1080/19443994.2012.671136
41. Agnihotri S, Mukherji S, Mukherji S (2012) Antimicrobial chitosan–PVA hydrogel as a nanoreactor and immobilizing matrix for silver nanoparticles. Appl Nanosci 2:179–188. https://doi.org/10.1007/s13204-012-0080-1
42. Horkay F, Tasaki I, Basser PJ (2000) Osmotic swelling of polyacrylate hydrogels in physiological salt solutions. Biomacromol 1:84–90. https://doi.org/10.1021/bm9905031
43. Okay O (2009) General properties of hydrogels. In: Gerlach G, Arndt K-F (eds) Hydrogel sensors and actuators, 1st edn. Springer, Berlin, pp 1–14
44. Allaker RP (2010) The use of nanoparticles to control oral biofilm formation. J Dent Res 89:1175–1186. https://doi.org/10.1177/0022034510377794
45. Jayasekara R, Harding I, Bowate I, Lonergan G (2005) Biodegradability of a selected range of polymers and polymer blends and standard methods for assessment of biodegradation synthetic. J Polym Environ 13:231–251. https://doi.org/10.1007/s10924-005-4758-2
46. Liu Y, Deng Y, Ping Chen, Duan M, Lin X, Zhang Y (2019) Biodegradation analysis of polyvinyl alcohol during the compost burial course. J Basic Microbiol 59:368–374
47. Hashimoto W, Mishima Y, Miyake O, Nankai H, Momma K, Murata K (2005) Biodegradation of Alginate, Xanthan, and Gellan Part 9. Miscellaneous biopolymers and biodegradation of polymers. Wiley, Hoboken

48. Jeon O, Bouhadir KH, Mansour JM, Alsberg E (2009) Photocrosslinked alginate hydrogels with tunable biodegradation rates and mechanical properties. Biomaterial 30:2724–2734. https://doi.org/10.1016/j.biomaterials.2009.01.034
49. Ilčin M, Holá O, BakajováB Kučerík J (2010) FT-IR study of gamma-radiation induced degradation of polyvinyl alcohol (PVA) and PVA/humic acids blends. J Radioanal Nucl Chem 283:9–13. https://doi.org/10.1007/s10967-009-0321-2
50. Jayasekara R, Harding I, Bowater I, Lonergan GT (2005) Biodegradability of a selected range of polymers and polymer blends and standard methods for assessment of biodegradation. J Polym Environ 13:231–251. https://doi.org/10.1007/s10924-005-4758-2
51. Jayasekara R, Harding I, Bowater I, Christieand GBY, Lonergan GT (2003) Biodegradation by Composting of Surface Modified Starch and PVA Blended Films. J Polym Environ 11:49–56. https://doi.org/10.1023/A:1024219821633
52. Luckachan GE, Pillai CKS (2011) Biodegradable polymers- a review on recent trends and emerging perspectives. J Polym Environ 19:637–676. https://doi.org/10.1023/A:1024219821633
53. Leja K, Lewandowicz G (2010) Polymer biodegradation and biodegradable polymers—a review. Pol J Environ Stud 19:255–266
54. Chiellini E, Corti A, D'Antone S, Solaro R (2003) Biodegradation of poly (vinyl alcohol) based materials. Prog Polym Sci 28:963–1014. https://doi.org/10.1016/S0079-6700(02)00149-1